Magnetostatic interaction in electrodeposited Ni/Au multilayer nanowire arrays*

Li-Zhong He(何丽忠), Li-Rong Qin(秦丽溶)†, Jian-Wei Zhao(赵建伟), Ying-Ying Yin(殷营营), Yu Yang(杨瑜), and Guo-Qing Li(李国庆)

School of Physical Science and Technology, Southwest University, Chongqing 400715, *China*

(Received 10 February 2016; revised manuscript received 12 April 2016; published online 25 June 2016)

Ordered Ni/Au multilayer nanowire arrays are successfully fabricated inside the nanochannels of anodic aluminum oxide template by pulse electrodeposition method. The thickness of the alternating layers is controlled to examine the magnetostatic interaction in Ni/Au multilayer nanowires. The magnetic easy axis parallel to the nanowires indicates that here the magnetostatic coupling along the wire axis dominates over the interactions perpendicular to the nanowires. However, the magnetostatic interaction between adjacent nanowires with larger magnetic layers is enhanced, leading to the existence of an optimum coercivity value.

Keywords: nanostructures, multilayers materials, metals, magnetic properties

PACS: 61.46.Km, 75.75.Cd **DOI:** 10.1088/1674-1056/25/8/086101

1. Introduction

Up to now, one-dimensional magnetic materials with novel special structures and morphologies have received much attention because of their potential applications in ultra-high density magnetic devices,[1] giant megnetoresistance (GMR) effect,[2,3] magnetoresistive spin-valves,[4] and a promising candidate of resistive switching.[5] One of them is multilayered ferromagnetic nanowire, which is particularly interesting because of the enhanced magnetic properties. Multilayered ferromagnetic nanowires can be obtained by a variety of approaches including colloidal synthesis,[6] vapor-solid-liquid (VLS),[7] template-assisted electrodeposition,[8] and other synthesis methods.[7] Among them, the template-assisted technique is a powerful approach because it is not only a simple and low cost method, but also has an accurate control over the lengths and placements of magnetic and nonmagnetic section of multilayer nanowires. Using a pulse electrodeposition method, many kinds of multilayer nanowires such as Ni/Cu,[9,10] CoNi/Cu,[11] NiFe/Cu,[12,13] Pt/Co,[1,14] and Pt/Ni[15] have been successfully fabricated experimentally. As a common nonmagnetic material, Au was often used to construct multilayer nanowires with Ni to optimize their magnetic properties. Clime *et al.* first reported the synthesis of Ni/Au multilayer nanowires.[16] Ishrat *et al.*[8] and Schelhas *et al.*[17] depicted the magnetic properties of Ni/Au multilayer nanowires from different viewpoints.

As is well known, the magnetic anisotropy of the nanowire arrays is mainly determined by the following three contributions:[18–20] the shape anisotropy, the magnetocrystalline anisotropy, and the magnetostatic coupling. For the multilayer nanowires, the magnetostatic coupling between the adjacent magnetic layers along the wire axis has been discussed many times. However, the magnetostatic coupling between the magnetic layers in adjacent nanowires has received only a little attention. In this paper, we design and fabricate the Ni/Au multilayer nanowires with the thickness of nonmagnetic Au layer equal to the distance of adjacent nanowire to make comparisons easier. The magnetic hysteresis loops are then measured, and the magnetostatic interaction is discussed in detail. Moreover, the Ni segment-length dependence of coercivity and squareness for the multilayer Ni/Au nanowires are also explored. Our results help us to have an in-depth understanding of the magnetic multilayer nanowires.

2. Experimental procedure

2.1. Preparation of AAO template

The AAO templates were homemade by a two-step anodization process as described in previous reports.[18,21] In brief, to obtain the high-quality of AAO templates, 99.999% Al sheets were annealed at 450 °C for 5 h and subsequently electropolished in a 1:9 volume mixture of perchloric acid and ethanol at 25 V to a mirror finish. Then, the first step of anodization was carried out at 45 V for 6 h in 0.3 mol/L oxalic acid electrolyte at about 8 °C. After the first step, the origin film was removed in a solution consisting of phosphoric acid (6 wt%) and chromic acid (1.8 wt%) at 60 °C for 9 h. The second anodization was performed under the same conditions. In this case, the distance between two adjacent channels would

*Project supported by the National Natural Science Foundation of China (Grant No. 11204246) and the Natural Science Foundation of CQCSTC (Grant No. cstc2014jcyjA50027).

†Corresponding author. E-mail: lrqin@swu.edu.cn

© 2016 Chinese Physical Society and IOP Publishing Ltd

be about 60 nm.

Subsequently, the remaining Al was extracted using $SnCl_4$ solution. To obtain the binary channels, the peeled AAO templates were immersed into a 6-wt% phosphoric acid solution 60 min at 30 °C to remove the barrier layer. For the electrodepositing target materials into the homogeneous and uniform pores of the AAO template, a thin gold layer was sputtered onto the back side of the AAO template to serve as the working electrode.

2.2. Fabrication of multilayer Ni/Au nanowires

The electrodeposition process of Ni/Au multilayer nanowires was performed in a three-electrode system. A graphite electrode was used as a counter electrode and an Ag/AgCl electrode was used as the reference electrode. The AAO template with gold layer served as the working electrode.[22] The electrodeposition single electrolyte used to deposit Au and Ni segments was composed of 5-g/L $HAuCl_4$–$4H_2O$, 10-g/L $NiCl_2$, 5-g/L $NiSO_4$, and 3-g/L H_3BO_3. The multilayer Ni/Au nanowires were deposited using a pulse signal that was adjusted to a deposition potential for each of the different target materials for a corresponding deposition time, such as (i) −0.35 V for 25 s for depositing Au layer, (ii) −1.3 V for 5 s, 10 s, 15 s, 25 s for depositing Ni layers with different thickness to obtain four kinds of nanowire samples, respectively. The total time of the electrochemical deposition was 20 min. During the electrodeposition, the electrodeposition electrolyte was continuously agitated by a magnetic stirrer.

2.3. Measurements

The phase composition of the prepared products was determined by x-ray Diffraction (XRD, D8 Advance). The morphologies and chemical compositions of fabricated Pt–Ni multilayered nanowires were characterized using a field-emission scanning electron microcopy (SEM, JSM 7100F) and high resolution transmission electron microscope (TEM, JEM 2010) equipped with energy dispersive x-ray spectrum (EDX). The magnetisms of the samples were analyzed by a vibrating sample magnetometer (VSM, ADE EV11).

3. Results and discussion

After removing the AAO templates, the morphologies of the products are investigated using SEM. As shown in Fig. 1(a), the low-magnification overhead view SEM image reveals that large quantities of well-aligned nanowires have been obtained. In this sample, the deposition time for each Ni layer and each Au layer are 5 s and 25 s, respectively. It can be seen that each nanowire has a well-faceted head and smooth surface. The average length of the nanowires is about 2.5 μm. Figure 1(b) is the side view of the multilayer nanowires. It shows that the average diameter of these nanowires is about 70 nm, corresponding to the diameter of the channels in the AAO template. The periodic separations between Au and Ni layers along the axis of the nanowires can also be clearly observed. The XRD pattern of the Ni/Au multilayer nanowires embedded in the AAO template is shown in Fig. 2. It indicates that the product consists of two compounds: one is face-centered cubic (fcc) structured Ni (JCPDS card no. 65-0380) and the other is fcc structured Au (JCPDS card no. 04-0784).

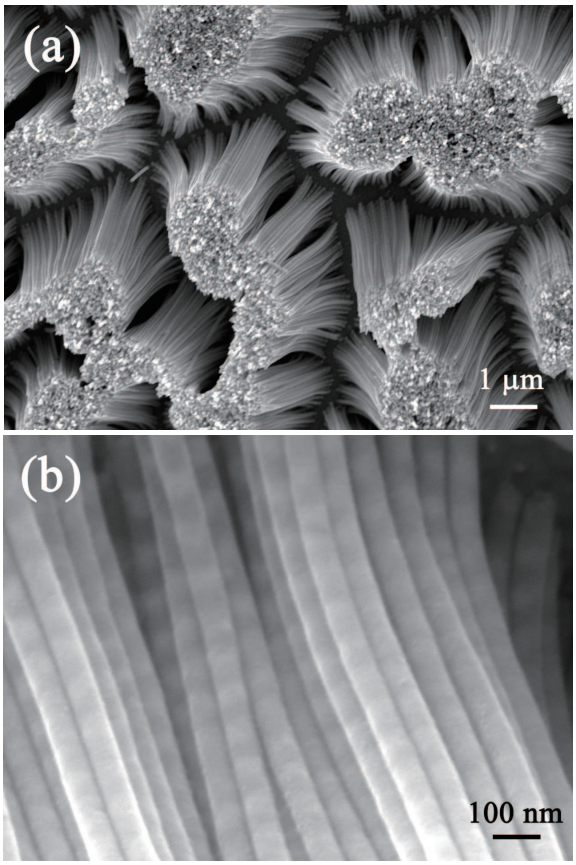


Fig. 1. (a) Typical low-magnification SEM image of Ni/Au multilayer nanowires, and (b) the high-magnification SEM image.

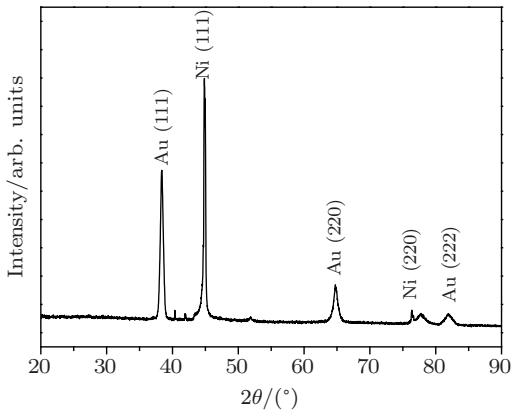


Fig. 2. XRD pattern of Ni/Au multilayer nanowires.

Further characterization of the multilayer nanowires was performed by TEM. Figure 3(a) shows a typical low-magnification TEM image of an individual nanowire behind

the template has been totally etched. The multilayer structure and reproducibility of the nanowire are clearly seen in this image. As indicated by arrows, the dark layers in the TEM image are those of Au while the lighter layers correspond to Ni, which is confirmed by the corresponding EDX analysis (Fig. 3(b)). Careful examination shows that the average thickness values of the Ni layer and the Au layer are 65 nm and 60 nm, respectively. It should be emphasized that the average thickness of the Au layers is equal to the distance between two adjacent nanowires, which would be favorable for the comparison of magnetostatic coupling between two different directions. The selected area electron diffraction (SAED) pattern taken from one Ni/Au nanowire is shown in the inset of Fig. 3(a). It shows a series of diffraction rings composed of some discrete diffraction spots, indicating that the Au layers and Ni layers are both polycrystalline. The HRTEM image of the interface area is shown in Fig. 3(c). It exhibits clear lattice fringes, revealing the formations of Au grains and Ni grains. The d-spacing of the left region denoted by parallel lines is 0.41 nm corresponding to the distance between the (001) planes of Au. But the d-spacing of the right region is 0.20 nm, which is close to the distance between the (111) planes of Ni. In our experiments, the thickness of the alternating layers can be easily controlled by varying the deposition time of each layer. But considering the fact that Clime *et al.*[16] have reported the synthesis of Ni/Au multilayer nanowires with the thickness of Ni layers lower than 30 nm, here we set purposely the deposition times of Ni layers to be 5 s, 10 s, 15 s, and 25 s, so that the corresponding thickness values of Ni layer would be 65 nm, 120 nm, 180 nm, and 300 nm as shown in Fig. 4. Their SAED patterns show a series of diffraction rings respectively, indicating that the prepared Ni/Au multilayer nanowires are all polycrystalline.

It has been investigated that the magnetic anisotropy of the nanowire arrays is mainly determined by the following three contributions:[18,19] i) the shape anisotropy resulting from the form effect of the individual wires, which will induce a magnetic easy axis parallel to the wire axis, ii) the magnetocrystalline anisotropy arising from bond anisotropy within the crystal lattice, and iii) the magnetostatic interaction. Specifically, for the multilayer nanowires, there are two types of magnetostatic couplings just as shown in Fig. 5. One is the magnetostatic coupling between the adjacent magnetic layers along the wire axis, which tends to develop a magnetic easy axis parallel to the wire axis. The other is the interaction between the adjacent nanowires, which tends to develop a magnetic easy axis perpendicular to the wire axis. This kind of interaction has received only a little attention in previous reports about multilayer nanowires. The overall magnetic nature of the multilayer nanowire arrays should be the result of the competition among the above contributions.

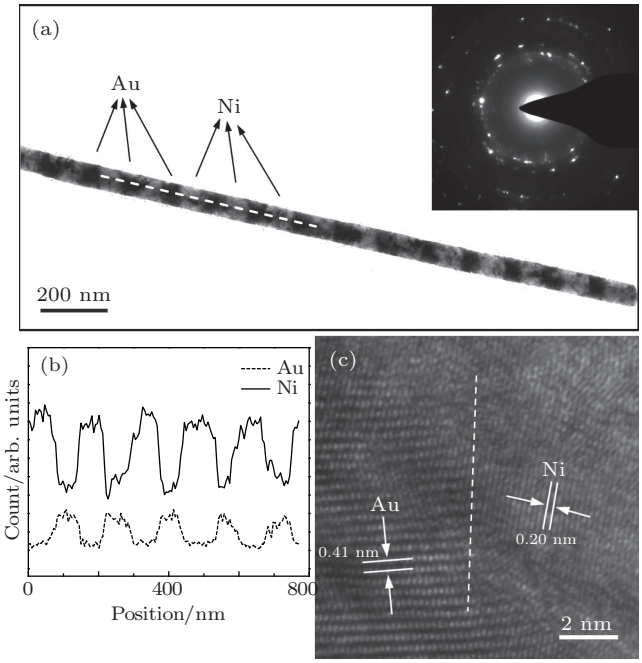


Fig. 3. (a) Typical TEM image of Ni/Au multilayer nanowires, Inset: corresponding SAED pattern, (b) elemental line scanning of Au and Ni composition along the nanowire, (c) the HRTEM image showing the interface between Au layer and Ni layer.

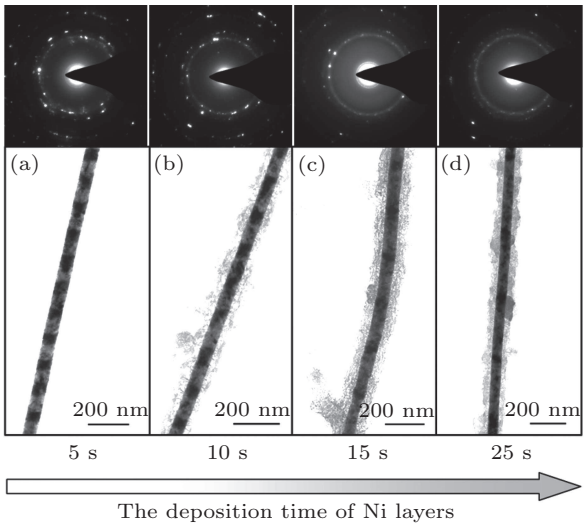


Fig. 4. TEM images and SAED patterns of Ni/Au multilayer nanowires when the deposition times of Ni layers are set to be (a) 5 s, (b) 10 s, (c) 15 s, (d) 25 s, respectively, and the deposition times of Au layers are all 25 s.

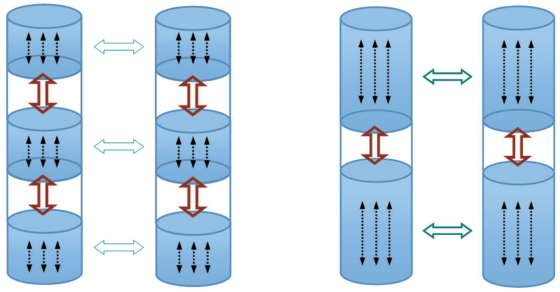


Fig. 5. (color online) Schematic diagram of the magnetostatic interactions. The wine solid arrows and olive solid arrows indicate the magnetostatic coupling; dot black arrows indicate the easy axis of each magnetic segment.

The magnetic hysteresis loops of Ni/Au multilayer nanowires embedded in the channels of AAO template are measured with the external magnetic field parallel and perpendicular to the long axis of the nanowires at room temperature and the results are shown in Fig. 6. On the whole, each of these arrays with different thickness of Ni layers possesses strong magnetic anisotropy with the easy axis parallel to the nanowires. The above properties are consistent with previously reported results about Ni,[23] Ni/Cu,[10] and Fe/Cu[24] nanowire arrays. As is well known, Ni is a magnetic material with very small magnetocrystalline anisotropy energy.[25] Furthermore, according to the structure analysis, the Ni layers in our products are polycrystalline, thus the magnetocrystalline anisotropy is not the reason for the easy axis parallel to the nanowires. The shape anisotropy always plays an important role and usually serves as explaining the phenomenon of the easy axis parallel to the magnetic nanowires. Nevertheless, it should be noted that for the Ni/Au nanowires with the shortest Ni layers (Fig. 6(a)), although the corresponding thickness of Ni layer is slightly less than the diameter of the nanowire with an aspect ratio of about 0.93, the easy axis is still parallel to the nanowires and the magnetic anisotropy is still strong. Obviously, this cannot be explained completely by the shape anisotropy of the Ni layer related mainly to the aspect ratio. Therefore, the anisotropy here should be attributed mainly to the magnetostatic coupling. The fact that the easy axis is parallel to the nanowires indicates that here the magnetostatic coupling between the adjacent magnetic layers along the wire axis dominates over the interactions among different nanowires. According to the structure analysis, we believe the interfaces between Ni and Au layers are approximately flat as shown schematically in Fig. 5, while the flanks of nanowires are obviously cylindrical surface. Because of the circular cross-section of Ni layers, there are no preferential in-plane alignment directions, which always exist in more standard rectangular cross-sections. This difference is likely to make the magnetostatic interaction stronger in the direction parallel to the wire axis. In other words, a head-to-tail alignment of magnetization along wire axis is energetically more favorable so as to minimize the magnetostatic energy of the system,[26] resulting in the easy axis parallel to the nanowires. As for those Ni/Au nanowires with larger Ni layer, of cause, the magnetostatic coupling still exists and combines with the shape anisotropy to result in the easy axis parallel to the nanowires. Moreover, we note that a weak bend appears in each central part of the hysteresis loop corresponding to the external magnetic field perpendicular to the nanowires in Fig. 6(d). A possible reason is that two ends and the centre of Ni layer has the inhomogeneous distribution of the magnetic moments caused by the shape anisotropy occurring in the longer Ni layer when the external magnetic field is perpendicular to the nanowires.

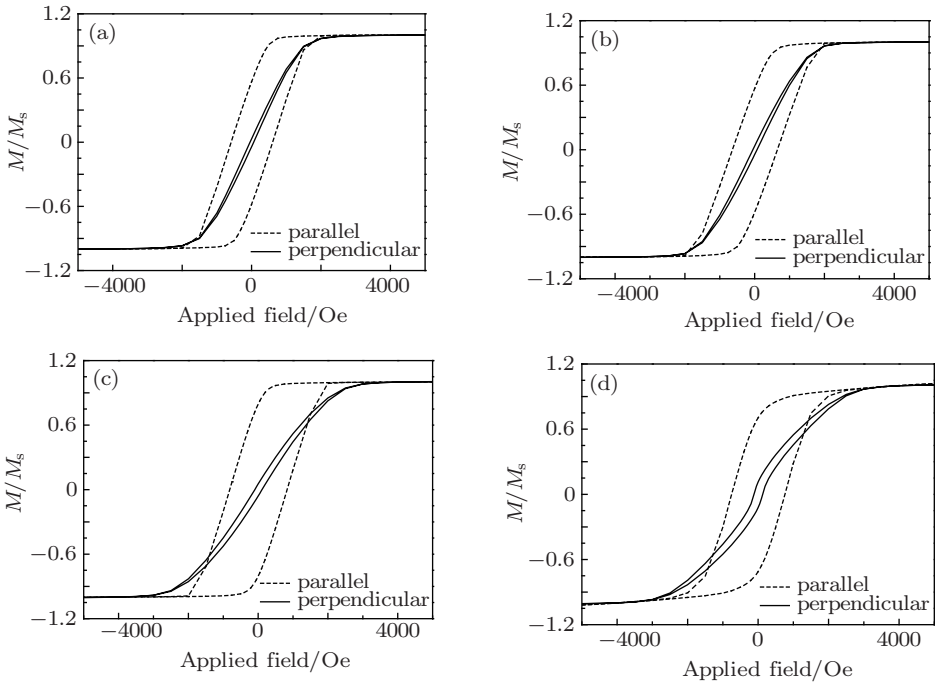


Fig. 6. Magnetization curves of Ni/Au nanowire arrays with applied magnetic field parallel and perpendicular to the wire axis, and depositing time $t_{Ni} = 5$ s (a), 10 s (b), 15 s (c), and 25 s (d).

As nonmagnetic material, the Au layers themselves have little effect on the magnetic properties of the multilayer nanowires. Schelhas *et al.*[17] have reported the magnetic coupling between Ni layers by controlling the lengths of Au layers in their multilayer Au–Ni nanowires. So the magnetizations of our samples are compared to show the effects of Ni layers with different thickness. In Fig. 7, the values of the coercivities and squareness of the nanowires for the

two field orientations are plotted each as a function of the deposition time of Ni layers. It is obvious that the coercivity initially increases to a maximum value of about 862.22 Oe (1 Oe = 79.5775 A·m^{-1}) as the thickness of Ni layer increases, and then decreases. Here, we can ascribe the initial increment to the shape anisotropy affected by increasing the aspect ratio of Ni layer. It is reported that if the aspect ratio of the Ni layer separated by nonmagnetic layer is less than 10, this Ni layer in multilayer nanowires is expected to be single domain.[9] So the subsequent decrease in the coercivity should not result from the effect of domain wall. In our previous work,[18] we have found the magnetostatic coupling among nanowires dominates over the shape anisotropy for the nanowires with an aspect ratio of about three. Because of this, we speculate here that the subsequent decrease in the coercivity may be related to the enhancement of magnetic coupling among the different nanowires with larger magnetic layers as illustrated in Fig. 5.[23] The effect of this coupling also lies in the change of the squareness. It can be seen from Fig. 7(b) that the squareness for the parallel field orientation exhibits the same variation behavior as that of the coercivity. Instead, the squareness for the perpendicular field orientation increases monotonically with increasing the angle between the magnetic field and the axis of the nanowires. Due to the contribution of the magnetic coupling among the different nanowires with larger magnetic layers, the squareness increases rather than reduces in the manner similar to the change of coercivity when the deposition time of Ni increases to 25 s. Besides, compared with the previous report about Ni/Au multilayer nanowires with the same diameter of 70 nm,[16] the coercivity presented here is great perhaps because of the larger aspect ratio of Ni layer. Due to the effect of multidomain structure, the coercivity of pure Ni nanowires has proven to be lower than that of Ni-based multilayer nanowires.[9] According to the change of the coercivity, it can be concluded that the relative optimum Ni layer thickness for the multilayer nanowires with diameter of 70 nm is about 180 nm corresponding to the aspect ratio of 2.6. As regards other kinds of multilayer nanowires, we consider that the differences in dimension, crystal structure, and defects also can influence the magnetic nature of the nanowire array thereby leading to a variety of specific results.

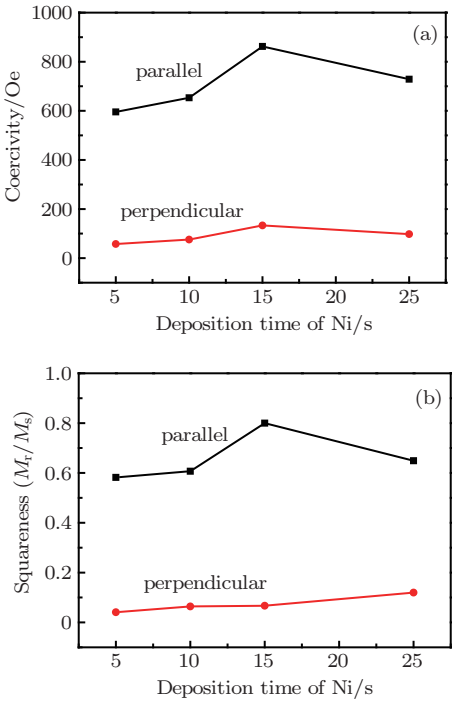


Fig. 7. (color online) Plots of (a) coercities and (b) squareness ratios in directions parallel and perpendicular to the nanowires versus deposition time of Ni layers.

4. Conclusions

In this work, we successfully synthesize Ni/Au multilayer nanowire arrays by pulse electrodeposition method. According to the measurements, magnetostatic coupling along the wire axis dominates over the interactions perpendicular to the nanowires, while the latter is enhanced for Ni/Au nanowires with larger magnetic layers. This change results in a relative optimum Ni layer thickness of about 180 nm. These experimental findings can be useful for assembling the future magnetic nanodevices.

References

[1] Choi J, Oh S J, Ju H and Cheon J 2005 *Nano Lett.* **5** 2179
[2] Baibich M N, Broto J M, Fert A, Nguyen F V D, Petroff E, Etienne P, Greuzet G, Friederich A and Chazelas J 1988 *Phys. Rev. Lett.* **61** 2472
[3] Prinz G A 1998 *Science* **282** 1660
[4] Dieny B 1994 *J. Magn. Magn. Mater.* **136** 335
[5] Herderick E D, Reddy K M, Sample R N, Draskovic T I and Padture N P 2009 *Appl. Phys. Lett.* **95** 203505
[6] Jun Y W, Choi J S and Cheon J 2006 *Angew. Chem. Int. Ed.* **45** 3414
[7] Hu J T, Odom T W and Lieber C M 1999 *ACC Chem. Res.* **32** 435
[8] Ishrat S, Maaz K, Lee K J, Jung M H and Kim G H 2014 *J. Solid State Chem.* **210** 116
[9] Liu R S, Chang S C, Hu S F and Huang C Y 2006 *Phys. Stat. Sol. (c)* **3** 1339
[10] Maleak N, Potpattanapol P, Bao N N, Ding J, Wongkokuo W, Tang I M and Thongmee S 2014 *J. Magn. Magn. Mater.* **354** 262
[11] Tang X T, Wang G C and Shima M 2007 *J. Magn. Magn. Mater.* **309** 188
[12] Krimpalis S, Dragos O G, Moga A E, Lupu N and Chiriac H J 2011 *Mater. Res.* **26** 1081
[13] Chiriac H, Ó VáRi T A and Pascariu P 2008 *J. Appl. Phys.* **103** 07D919
[14] Peng Y, Cullis T, Luxmoore I and Inkson B 2011 *Nanotechnology* **22** 245709
[15] Liu F, Lee J Y and Zhou W 2004 *J. Phys. Chem.* **108** 17959
[16] Clime L, Zhao S Y, Chen P, Normandin F, Roberge H and Veres T 2007 *Nanotechnology* **18** 435709
[17] Schelhas L T, Banholzer M J, Mirkin C A and Tolbert S H 2015 *J. Magn. Magn. Mater.* **379** 239
[18] Qin L R, Zhao J W, Guo Q, Yan Z K, Mu F, Chen P and Li G Q 2013 *Physica E* **50** 17
[19] Han G C, Zong B Y, Luo P and Wub Y H 2003 *J. Appl. Phys.* **93** 9202
[20] Zhang J J, Li Z Y, Zhang H M, Hou X and Sun H Y 2013 *Chin. Phys. B* **22** 087805
[21] Yan Z K, Zhao J W, Qin L R, Mu F, Wang P and Feng X N 2013 *Microchim. Acta* **180** 145
[22] Cho J U, Liu Q X, Min J H, Ko S P and Kim Y K 2006 *J. Magn. Magn. Mater.* **304** e213
[23] Lavín R, Denardin J C, Escrig J, Altbir D, Cortés A and Gómez H 2009 *J. Appl. Phys.* **106** 103903
[24] Almasi-Kashi M, Ramazani A, Kheyri F and Jafari-Khamse E 2014 *Mater. Chem. Phys.* **144** 230
[25] Tian F, Zhu J and Wei D 2007 *J. Phys. Chem. C* **111** 12669
[26] Tang X T, Wang G C and Shima M 2006 *IEEE T. Magn.* **42** 2975